NEURAL REGENERATION RESEARCH
July 2016, Volume 11, Issue 7
www.nrronline.org

RESEARCH ARTICLE

Dose response and time course of manganese-enhanced magnetic resonance imaging for visual pathway tracing *in vivo*

Wei-ling Wang[1, 2], Hui Xu[3], Ying Li[4], Zhi-zhong Ma[4], Xiao-dong Sun[5, *], Yun-tao Hu[1, 4, *]

1 Department of Ophthalmology, Beijing Tsinghua Changgung Hospital, Tsinghua University Medical Center, Beijing, China
2 Department of Ophthalmology, General Hospital of Ningxia Medical University, Yinchuan, Ningxia Hui Autonomous Region, China
3 Department of Radiology, Peking University Third Hospital, Beijing, China
4 Peking University Eye Center, Peking University Third Hospital, Key Laboratory of Vision Loss and Restoration, Ministry of Education, Beijing, China
5 Department of Ophthalmology, Shanghai Jiao Tong University Affiliated First People's Hospital, Shanghai, China

How to cite this article: *Wang WL, Xu H, Li Y, Ma ZZ, Sun XD, Hu YT (2016) Dose response and time course of manganese-enhanced magnetic resonance imaging for visual pathway tracing in vivo. Neural Regen Res 11(7):1185-1190.*

Funding: *This study was supported by a grant from the National Basic Research Program of China (973 Program), No. 2011CB707506; the Seed Fund from the Peking University Third Hospital of China, No. YZZ08-9-13; and the Linghu Fund from the Peking University Third Hospital of China, No. 64508-01.*

Graphical Abstract

Manganese-enhanced magnetic resonance imaging (MRI) is a viable method for temporospatial tracing visual pathway *in vivo*

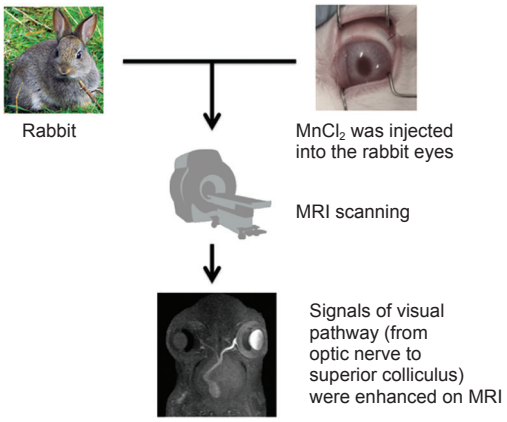

Correspondence to:
Yun-tao Hu or Xiao-dong Sun, ythu@mail.tsinghua.edu.cn or xdsun@sjtu.edu.cn.

orcid:
0000-0003-4663-0684 (Yun-tao Hu)

doi: *10.4103/1673-5374.187065*

Accepted: *2016-06-12*

Abstract

Axonal tracing is useful for detecting optic nerve injury and regeneration, but many commonly used methods cannot be used to observe axoplasmic flow and synaptic transmission *in vivo*. Manganese (Mn^{2+})-enhanced magnetic resonance imaging (MEMRI) can be used for *in vivo* longitudinal tracing of the visual pathway. Here, we explored the dose response and time course of an intravitreal injection of $MnCl_2$ for tracing the visual pathway in rabbits *in vivo* using MEMRI. We found that 2 mM $MnCl_2$ enhanced images of the optic nerve but not the lateral geniculate body or superior colliculus, whereas at all other doses tested (5–40 mM), images of the visual pathway from the retina to the contralateral superior colliculus were significantly enhanced. The images were brightest at 24 hours, and then decreased in brightness until the end of the experiment (7 days). No signal enhancement was observed in the visual cortex at any concentration of $MnCl_2$. These results suggest that MEMRI is a viable method for temporospatial tracing of the visual pathway *in vivo*. Signal enhancement in MEMRI depends on the dose of $MnCl_2$, and the strongest signals appear 24 hours after intravitreal injection.

Key Words: *nerve regeneration; manganese; magnetic resonance imaging; visual pathway; optic nerve; tracing; in vivo; intravitreal injection; time; dose; neural regeneration*

Introduction

Axonal tracing is a valuable tool for detecting optic nerve injury and regeneration. Some axonal tracing methods require the use of histological techniques, which cannot be used to observe axoplasmic flow or synaptic transmission *in vivo* because they require the experimental animals to be killed prior to tissue sectioning. Such techniques include the use of herpes simplex virus, indocyanine green, carbocyanine fast DiI, and biotinylated dextran (Rajakumar et al., 1993; Tillet et al., 1993; Mombaerts et al., 1996; Sun et al., 1996; Norgren and Lehman, 1998; Reiner et al., 2000; Sparks et al., 2000; Paques et al., 2003).

Manganese (Mn^{2+}) is a calcium analog and a paramagnetic contrast agent for MRI. It shortens the relaxation constant T1, resulting in an image with enhanced signal contrast in the tract or cortical regions containing it. Mn^{2+} is a trans-synaptic tracer that is taken up into neurons *via* voltage-gated Ca^{2+} channels, packaged into vesicles, and transported down the axon in a microtubule-dependent manner (Narita et al., 1990; Takeda et al., 1998; Pautler and Koretsky, 2002). Mn^{2+}-enhanced magnetic resonance imaging (MEMRI) makes it feasible to trace the visual pathway longitudinally in living animals. The resulting image, showing elevated signal intensity in the Mn^{2+}-containing visual pathway, demonstrates that intravitreal Mn^{2+} can be taken up by retinal ganglion cells (RGCs) and transported along axons to the cortex (Watanabe et al., 2001; Ryu et al., 2002; Thuen et al., 2005; Pautler, 2006; Zhang et al., 2010b; Lin et al., 2014), thus allowing the visual pathway to be viewed on MRI images. MEMRI has been used to study the connections and functional properties of the songbird vocal control system (Van der Linden et al., 2002; Tindemans et al., 2003; Van Meir et al., 2004) and the visual pathway of mice and rats (Lin et al., 2001; Watanabe et al., 2001; Yamada et al., 2008; Chan et al., 2011). In addition, the technique has been used to observe chronic glaucoma, radiation-induced optic neuropathy, and optic nerve injury and regeneration in mice, rats, frogs and fish (Ryu et al., 2002; Chan et al., 2008; Thuen et al., 2009; Sandvig et al., 2011).

Sandvig et al. (2011) demonstrated that MEMRI is a viable method for serial *in vivo* monitoring of normal, induced, and spontaneously regenerating optic nerve axons in different species. Lowe et al. (2008) and Olsen et al. (2010) observed that Mn^{2+} tract tracing was dose-, space- and time-dependent in mice and rats. Furthermore, Olsen et al. (2010) suggested that the entry of Mn^{2+} into RGC axons is rate-dependent and not directly proportional to the vitreal concentration in rats. Lowe et al. (2008) examined different concentrations of Mn^{2+} for MEMRI tract tracing in mice. They found that the concentrations used for optimal tract tracing might actually block neuronal activity. In our previous studies (Zhang et al., 2010a; Luo et al., 2012), we showed that intravitreal injection of $MnCl_2$ induces retinal cell damage from concentrations of 20 mM and 25 mM or more, in rabbits and rats, respectively. This species difference may be because the volume of $MnCl_2$ injected into the vitreous body was greater in rabbits than in rats.

The rabbit is a useful animal model for studying optic nerve injury and regeneration. However, to our knowledge, there have been no reports of the use of MEMRI for displaying the visual pathway in rabbits *in vivo*. Therefore, in the present study, we characterized the dose response and time course of intravitreal $MnCl_2$ injections for visual pathway image enhancement in rabbits *in vivo*.

Materials and Methods

Animals

We used 36 clean male and female pigmented rabbits, weighing 2–2.5 kg. All experiments were carried out in accordance with the Association for Research in Vision and Ophthalmology Statement for the Use of Animals in Ophthalmic and Vision Research. Precautions were taken to minimize suffering and the number of animals used in each experiment.

MEMRI

The rabbits were equally and randomly divided into six groups, irrespective of sex, and were anesthetized by intramuscular injection of a mixture of ketamine hydrochloride (15 mg/kg; Fujian Thou Farmland Pharmaceutical Co., Ltd., Gutian, Fujian Province, China) and xylazine hydrochloride (15 mg/kg; Jilin University of Veterinary Medicine, Changchun, Jilin Province, China).

Each group received a 25-μL injection of an aqueous solution of $MnCl_2$ (2, 5, 10, 15, 20 or 40 mM; Tianjin Kemiou Chemical Reagent Co., Ltd., Tianjin, China) into the vitreous body of the left eye through the pars plana (2 mm posterior to the limbus). The needle was withdrawn slowly to minimize reflux after injection. An anterior chamber tap was used to balance the intraocular pressure. The right eye served as the non-injected control.

Serial MRI images of the visual pathway were taken using a 1.5T Sonata MR System (Siemens, Erlangen, Germany), with a maximum gradient capability of 40 mT/m, at 4, 6, 8, 12, and 24 hours, and 2, 4, and 7 days after $MnCl_2$ administration. A flexible coil for animals (Chen Guang Medical Science Co., Shanghai, China) was used to obtain all images and to compile a three-dimensional stereoscopic image of the brain. Each animal had its head placed inside the coil and was fixed on a custom-made frame to prevent movement. The following imaging parameters were used: three-dimensional, fast, low-angle shot sequence; matrix dimensions = 256 × 256; slice thickness = 0.5 mm; repetition time = 10 ms; echo time = 3.59 ms; average = 6 times; field of view = 90 mm. All data were uploaded to an image workstation (Leonardo, Siemens) and image reconstruction was performed using Siemens Standard 12 dirs software.

MRI data analysis

Images were reconstructed using the maximum intensity projection technique (slice thickness = 10 mm, level distance = 3 mm). To quantify Mn^{2+} enhancement in the

Table 1 Comparisons of visual pathway signal-to-noise ratios in the injected *vs.* control eye 24 hours after injection with various concentrations of $MnCl_2$

$MnCl_2$ (mM)	Left eye (injected)			Right eye (non-injected control)		
	Optic nerve	Lateral geniculate body	Superior colliculus	Optic nerve	Lateral geniculate body	Superior colliculus
2	86.6±2.8*	54.2±2.9	53.8±3.0	57.3±2.5	54.2±1.3	54.4±1.5
5	101.3±3.7$^{*\#}$	70.2±2.6$^{*\#}$	71.0±3.2$^{*\#}$	51.6±2.2	49.2±1.9	58.9±1.8
10	113.8±2.8$^{*\#}$	73.6±3.0$^{*\#}$	62.4±2.2$^{*\#}$	62.4±1.8	58.8±2.1$^{\#}$	55.3±2.1$^{\#}$
15	137.3±3.3$^{*\#}$	93.5±3.3$^{*\#}$	92.3±2.7$^{*\#}$	79.4±3.6$^{\#}$	73.6±2.6$^{\#}$	62.6±2.6$^{\#}$
20	140.6±2.4$^{*\#}$	94.1±2.5$^{*\#}$	85.5±4.5$^{*\#}$	60.3±1.8$^{\#}$	61.5±2.5$^{\#}$	59.8±2.1$^{\#}$
40	157.6±3.2$^{*\#}$	107.1±4.0$^{*\#}$	98.8±2.7$^{*\#}$	68.2±2.8$^{\#}$	61.9±3.5$^{\#}$	52.4±2.8$^{\#}$

Data are expressed as the mean ± SD. Factorial analysis of variance was used with homogenous variances, with the least significant difference *post hoc* test. Dose: $F = 46.630$, $P = 0.000$; eyes: $F = 222.824$, $P = 0.000$; interaction: $F = 18.612$, $P = 0.000$. *$P < 0.05$, *vs.* right eye; #$P < 0.05$, *vs.* 2 mM $MnCl_2$.

visual pathway, the region of interest (ROI) was selected by manually drawing along the Mn^{2+}-enhanced and contralateral non-enhanced visual pathways. The ROI included the optic nerve, lateral geniculate body and superior colliculus. The mean signal intensity of the ROI was measured, and the signal-to-noise ratio (SNR) was calculated using the following formula: SNR = S/SD, where S is the signal intensity in the ROI of the Mn^{2+}-enhanced area or the contralateral isotopic non-enhanced area of the visual pathway, and SD is the standard deviation of the background noise. The data were collected by one investigator who did not know which eye had received the intravitreal $MnCl_2$ injection.

Statistical analysis

Data were analyzed using SPSS version 15.0 (SPSS Inc., Chicago, IL, USA), and were expressed as the mean ± SD unless otherwise indicated. Percent-percent plots were used to test for normality, and data were considered normally distributed if a linear trend appeared on the scatter diagram. For comparisons of SNRs in the two sides in the optic nerve, lateral geniculate body and superior colliculus, homogeneity tests of variances were performed. A factorial analysis of variance was used when the variances were homogeneous, and the least significant difference *post hoc* test was used to perform specific comparisons. Regression analysis of the relationship between the optic nerve SNR and $MnCl_2$ concentration was carried out by curve fitting, and the fitted equation was analyzed using the *F* test. A 95% significance level was used in all statistical tests.

Results

Dose response of MEMRI in the visual pathway

The dose-response relationship of intravitreal $MnCl_2$ and MEMRI was observed 24 hours after injection (**Table 1**, **Figure 1**). The visual pathway from the retina to the contralateral superior colliculus was enhanced significantly at $MnCl_2$ concentrations of 5–40 mM ($P < 0.05$), and the whole visual pathway was observed clearly at 10–40 mM. However, enhancement of the MRI signal was not detected in the visual cortex at any concentration. At 2 mM, the SNR of the optic nerve ipsilateral to the injected eye was significantly greater than that of the control eye ($P < 0.05$). However, no enhancement was observed in the lateral geniculate body or superior colliculus contralateral to the injected eye at this low concentration ($t = 0.04$ and 0.22, respectively; $P > 0.05$ *vs.* control eye; **Table 1**, **Figure 1**). In a preliminary study, we found no visual pathway enhancement at $MnCl_2$ concentrations lower than 2 mM. Comparing the SNR at each concentration with that at 2 mM showed that bilateral contrast enhancement occurred at 5–40 mM in the optic nerve, and at 10–40 mM $MnCl_2$ in the lateral geniculate body and superior colliculus.

Regression analysis revealed that the SNR of the optic nerve increased with increasing concentrations of Mn^{2+} ($R^2 = 0.984$, $P = 0.000$; **Figure 2**).

Time course of MEMRI in the visual pathway

SNR was measured in the optic nerve to observe the time course of MEMRI at 5, 10, 15, 20, and 40 mM $MnCl_2$. SNR in the optic nerve began to increase significantly 4 hours after injection. The maximum SNR was observed at 24 hours, after which it reduced, nearing control values by 7 days after injection (**Figure 3**).

In the optic chiasm, SNR enhancement was detected at 6 hours after intravitreal $MnCl_2$ injection, in the lateral geniculate body at 8 hours, and in the contralateral superior colliculus at 12 hours. The whole visual pathway was clear 24 hours after injection (**Figure 4**).

Discussion

RGCs are located in the inner layer of the retina and their axons form the optic nerve, which leaves the eye at the lamina cribrosa. In rodents, the majority of RGC axons in the optic nerve decussate in the optic chiasm and project into the contralateral optic tract to subcortical targets, including the thalamic lateral geniculate nucleus, midbrain pretectum, and superior colliculus (Voogd, 1998; Isenmann et al., 2003; Harvey, 2014; So et al., 2014). For visual pathway tracing *in vivo*, Mn^{2+} is taken up by RGCs through voltage-gated Ca^{2+} channels after intravitreal injection (Narita et al., 1990). Intracellularly, Mn^{2+} is distributed in vesicles and transported

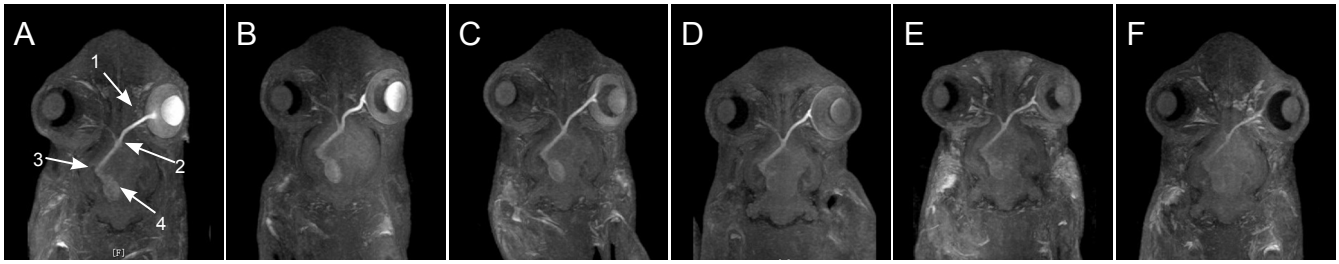

Figure 1 MRI images 24 hours after intravitreal injection with various concentrations of $MnCl_2$ (2–40 mM).
(A–F) $MnCl_2$ concentration: 40, 20, 15, 10, 5, 2 mM, respectively. $MnCl_2$ dose-dependently enhanced the visual pathway from the retina to the contralateral superior colliculus. Arrows 1, 2, 3, 4 represent optic nerve, optic chiasm, lateral geniculate body, and superior colliculus, respectively.

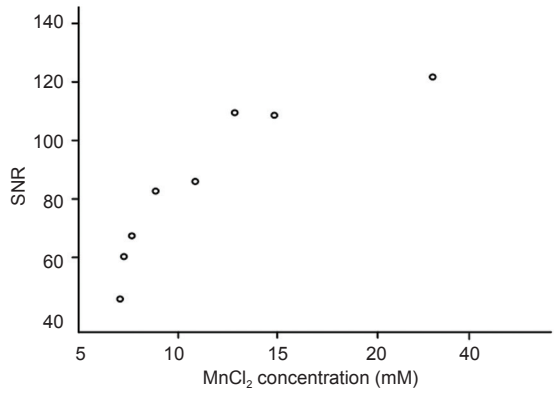

Figure 2 Positive correlation between optic nerve SNR and $MnCl_2$ concentration.
Regression analysis of the relationship between the SNR in the optic nerve and $MnCl_2$ concentration was carried out by curve fitting. The fitted equation was analyzed using an F test. $y = 66.234 + 24.269 \ln(x)$, where y = optic nerve SNR and x = $MnCl_2$ concentration. $F = 374.15$, $P = 0.000$, $R^2 = 0.984$. SNR: Signal-to-noise ratio.

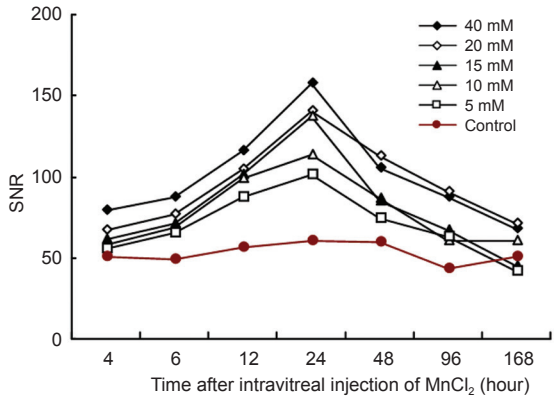

Figure 3 Time course of SNR in the optic nerve after intravitreal injection of different concentrations of $MnCl_2$.
Concentration: $F = 90.596$, $P = 0.000$; time: $F = 305.14$, $P = 0.000$; interaction: $F = 5.137$, $P = 0.000$. SNR: Signal-to-noise ratio.

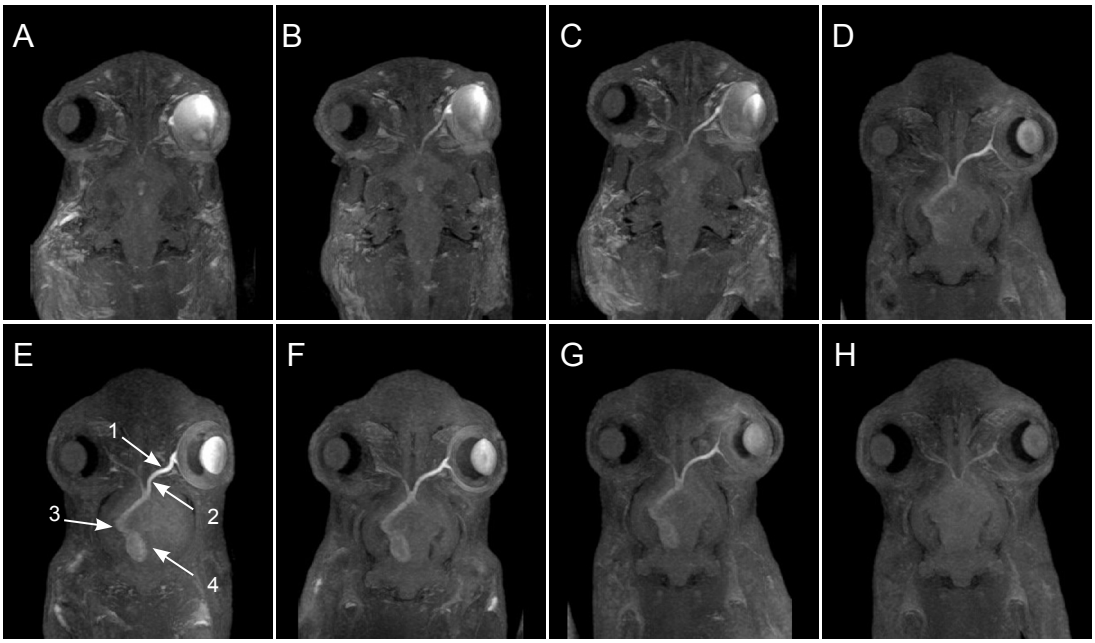

Figure 4 MRI of the visual pathway at various time points after intravitreal injection of 20 mM $MnCl_2$.
(A–H) 4, 6, 8 12, 24 hours, 2, 4, and 7 days, respectively. Arrows 1, 2, 3, 4 represent optic nerve, optic chiasm, lateral geniculate body, and superior colliculus, respectively.

anterogradely along axonal microtubules. Several studies have shown that Mn^{2+} transport is reduced after administration of the microtubule-disrupting agent colchicine (Sloot and Gramsbergen, 1994; Pautler and Koretsky, 2002). When Mn^{2+} reaches a synapse, it is released into the synaptic cleft where it may be taken up by Ca^{2+} channels on the postsynaptic membrane (Takeda et al., 1998; Saleem et al., 2002).

We used MEMRI to observe the visual pathway in rabbits and revealed the dose-response relationship and time course of signal enhancement after intravitreal injection of $MnCl_2$. In the range of 5–40 mM, 25 μL of $MnCl_2$ increased MRI signal along the visual pathway from the retina to the contralateral superior colliculus. SNR in the optic nerve increased with increasing concentrations of Mn^{2+}. At 2 mM, Mn^{2+} enhanced the signal in the optic nerve, but not in the lateral geniculate body or superior colliculus contralateral to the injection. These results demonstrate that signal enhancement by MEMRI is dose-dependent. In the range of Mn^{2+} concentrations tested (2–40 mM), we did not find a saturation effect.

Contrast enhancement was not observed in the lateral geniculate body or superior colliculus ipsilateral to the injection, although the data showed that the SNRs of these parts of the visual pathway were significantly elevated after 10–40 mM $MnCl_2$ compared with 2 mM. This suggests that most axons of the optic nerve run to the contralateral side after the optic chiasm, and only a minority remain on the ipsilateral side. The concentration of $MnCl_2$ reaching the lateral geniculate body and superior colliculus ipsilateral to the injection was not sufficient to enhance the MRI contrast signals in these areas. Interestingly, SNR in the contralateral optic nerve was elevated at 15–40 mM compared with 2 mM; this might be the result of Mn^{2+} diffusion in the optic chiasm.

Consistent with previous reports, we found no trans-synaptic movement of Mn^{2+} to the visual cortex or any enhancement of the MRI signal here (Silva et al., 2004; Thuen et al., 2005), despite evidence that Mn^{2+} can traverse the synapse in the rodent olfactory pathway (Pautler et al., 1998; Pautler and Koretsky, 2002). Watanabe et al. (2001) suggested that the reason for a lack of trans-synaptic movement of Mn^{2+} ions in the visual pathway was because of dilution of local Mn^{2+} that had traveled a long distance from the retina to the lateral geniculate body and superior colliculus, leaving too few Mn^{2+} ions transported to the visual cortex to cause a change of signal. In addition, Henriksson et al. (1999) showed that the uptake of Mn^{2+} into the olfactory epithelium and its transfer to the olfactory bulb along the primary olfactory neurons is a saturable process. Therefore, it is reasonable to speculate that Mn^{2+} uptake in RGCs and its transfer along their axons is a similarly saturable process, and the local Mn^{2+} concentration may be the limiting factor in determining MEMRI signal contrast for neuronal tracing (Watanabe et al., 2001).

In our time course study, the signals of optic nerves were enhanced 4 hours after Mn^{2+} injection at concentrations of 5–40 mM. Each part of the visual pathway, from the optic nerve head to the superior colliculus, was enhanced in succession over 12 hours. The maximum SNR in the visual pathway was observed at 24 hours, after which it decreased until the end of the experiment. Optic nerve signals recovered to control levels at 7 days. These results demonstrated that Mn^{2+} accumulated in the visual pathway and reached a peak at 24 hours, independent of concentration.

In summary, we have investigated the changes in MEMRI signal contrast with dose and time for tracing the visual pathway in rabbits. Mn^{2+} at 5–40 mM significantly enhanced the signal in the visual pathway from the optic nerve to the superior colliculus in T1-weighted images. The best time for observation was 24 hours after intravitreal injection of Mn^{2+}. These results are in line with those of previous studies in rats and mice (Natt et al., 2002; Lowe et al., 2008; Olsen et al., 2010), and provide further evidence that MEMRI is a useful technique for studying the axonal function of the optic nerve in many species *in vivo*.

Acknowledgments: *We are very grateful to Dr. Kang Feng from Peking University Eye Center, Peking University Third Hospital in China to help us in data analysis.*

Author contributions: *WLW performed the experiment and wrote the paper. HX and YL performed the experiment and discussed data. ZZM and XDS analyzed data and served as principle investigators. YTH participated in study design and wrote the paper. All authors approved the final version of the paper.*

Conflicts of interest: *None declared.*

Plagiarism check: *This paper was screened twice using Cross-Check to verify originality before publication.*

Peer review: *This paper was double-blinded and stringently reviewed by international expert reviewers.*

References

Chan KC, Fu QL, Hui ES, So KF, Wu EX (2008) Evaluation of the retina and optic nerve in a rat model of chronic glaucoma using in vivo manganese-enhanced magnetic resonance imaging. Neuroimage 40:1166-1174.

Chan KC, Li J, Kau P, Zhou IY, Cheung MM, Lau C, Yang J, So KF, Wu EX (2011) In vivo retinotopic mapping of superior colliculus using manganese-enhanced magnetic resonance imaging. Neuroimage 54:389-395.

Harvey AR (2014) Gene therapy and the regeneration of retinal ganglion cell axons. Neural Regen Res 9:232-233.

Henriksson J, Tallkvist J, Tjälve H (1999) Transport of manganese via the olfactory pathway in rats: dosage dependency of the uptake and subcellular distribution of the metal in the olfactory epithelium and the brain. Toxicol Appl Pharmacol 156:119-128.

Isenmann S, Kretz A, Cellerino A (2003) Molecular determinants of retinal ganglion cell development, survival, and regeneration. Prog Retin Eye Res 22:483-543.

Lin CP, Tseng WY, Cheng HC, Chen JH (2001) Validation of diffusion tensor magnetic resonance axonal fiber imaging with registered manganese-enhanced optic tracts. Neuroimage 14:1035-1047.

Lin TH, Chiang CW, Trinkaus K, Spees WM, Sun P, Song SK (2014) Manganese-enhanced MRI (MEMRI) via topical loading of Mn(2+) significantly impairs mouse visual acuity: a comparison with intravitreal injection. NMR Biomed 27:390-398.

Lowe AS, Thompson ID, Sibson NR (2008) Quantitative manganese tract tracing: dose-dependent and activity-independent terminal labelling in the mouse visual system. Nmr Biomed 21:859-867.

Luo L, Xu H, Li Y, Du Z, Sun X, Ma Z, Hu Y (2012) Manganese-enhanced MRI optic nerve tracking: effect of intravitreal manganese dose on retinal toxicity. Nmr Biomed 25:1360-1368.
Mombaerts P, Wang F, Dulac C, Chao SK, Nemes A, Mendelsohn M, Edmondson J, Axel R (1996) Visualizing an olfactory sensory map. Cell 87:675-686.
Narita K, Kawasaki F, Kita H (1990) Mn and Mg influxes through Ca channels of motor nerve terminals are prevented by verapamil in frogs. Brain Res 510:289-295.
Natt O, Watanabe T, Boretius S, Radulovic J, Frahm J, Michaelis T (2002) High-resolution 3D MRI of mouse brain reveals small cerebral structures in vivo. J Neurosci Methods 120:203-209.
Norgren RB, Lehman MN (1998) Herpes simplex virus as a transneuronal tracer. Neurosci Biobehav Rev 22:695-708.
Olsen Ø, Kristoffersen A, Thuen M, Sandvig A, Brekken C, Haraldseth O, Goa PE (2010) Manganese transport in the rat optic nerve evaluated with spatial- and time-resolved magnetic resonance imaging. J Magn Reson Imaging 32:551-560.
Paques M, Genevois O, Régnier A, Tadayoni R, Sercombe R, Gaudric A, Vicaut E (2003) Axon-tracing properties of indocyanine green. Arch Ophthalmol 131:367-370.
Pautler RG (2006) Biological applications of manganese-enhanced magnetic resonance imaging. Methods Mol Med 124:365-386.
Pautler RG, Koretsky AP (2002) Tracing odor-induced activation in the olfactory bulbs of mice using manganese-enhanced magnetic resonance imaging. Neuroimage 16:441-448.
Pautler RG, Silva AC, Koretsky AP (1998) In vivo neuronal tract tracing using manganese-enhanced magnetic resonance imaging. Magn Reson Med 40:740-748.
Rajakumar N, Elisevich K, Flumerfelt BA (1993) Biotinylated dextran: a versatile anterograde and retrograde neuronal tracer. Brain Res 607:47-53.
Reiner A, Veenman CL, Medina L, Jiao Y, Del Mar N, Honig MG (2000) Pathway tracing using biotinylated dextran amines. J Neurosci Methods 103:23-37.
Ryu S, Brown SL, Kolozsvary A, Ewing JR, Kim JH (2002) Noninvasive detection of radiation-induced optic neuropathy by manganese-enhanced MRI. Radiat Res 157:500-505.
Saleem KS, Pauls JM, Augath M, Trinath T, Prause BA, Hashikawa T, Logothetis NK (2002) Magnetic resonance imaging of neuronal connections in the macaque monkey. Neuron 34:685-700.
Sandvig A, Sandvig I, Berry M, Olsen Ø, Pedersen TB, Brekken C, Thuen M (2011) Axonal tracing of the normal and regenerating visual pathway of mouse, rat, frog, and fish using manganese-enhanced MRI (MEMRI). J Magn Reson Imaging 34:670-675.
Silva AC, Lee JH, Aoki I, Koretsky AP (2004) Manganese-enhanced magnetic resonance imaging (MEMRI): methodological and practical considerations. Nmr Biomed 17:532-543.
Sloot WN, Gramsbergen JB (1994) Axonal transport of manganese and its relevance to selective neurotoxicity in the rat basal ganglia. Brain Res 657:124-132.
So KF, Leung MC, Cui Q (2014) Effects of low level laser treatment on the survival of axotomized retinal ganglion cells in adult Hamsters. Neural Regen Res 9:1863-1869.
Sparks DL, Lue LF, Martin TA, Rogers J (2000) Neural tract tracing using Di-I: a review and a new method to make fast Di-I faster in human brain. J Neurosci Methods 103:3-10.
Sun N, Cassell MD, Perlman S (1996) Anterograde, transneuronal transport of herpes simplex virus type 1 strain H129 in the murine visual system. J Virol 70:5405-5413.
Takeda A, Kodama Y, Ishiwatari S, Okada S (1998) Manganese transport in the neural circuit of rat CNS. Brain Res Bull 45:149-152.
Thuen M, Singstad TE, Pedersen TB, Haraldseth O, Berry M, Sandvig A, Brekken C (2005) Manganese-enhanced MRI of the optic visual pathway and optic nerve injury in adult rats. J Magn Reson Imaging 22:492-500.
Thuen M, Olsen O, Berry M, Pedersen TB, Kristoffersen A, Haraldseth O, Sandvig A, Brekken C (2009) Combination of Mn(2+)-enhanced and diffusion tensor MR imaging gives complementary information about injury and regeneration in the adult rat optic nerve. J Magn Reson Imaging 29:39-51.
Tillet Y, Batailler M, Thibault J (1993) Neuronal projections to the medial preoptic area of the sheep, with special reference to monoaminergic afferents: immunohistochemical and retrograde tract tracing studies. J Comp Neurol 330:195-220.
Tindemans I, Verhoye M, Balthazart J, Van Der Linden A (2003) In vivo dynamic ME-MRI reveals differential functional responses of RA- and area X-projecting neurons in the HVC of canaries exposed to conspecific song. Eur J Neurosci 18:3352-3360.
Van der Linden A, Verhoye M, Van Meir V, Tindemans I, Eens M, Absil P, Balthazart J (2002) In vivo manganese-enhanced magnetic resonance imaging reveals connections and functional properties of the songbird vocal control system. Neuroscience 112:467-474.
Van Meir V, Verhoye M, Absil P, Eens M, Balthazart J, Van der Linden A (2004) Differential effects of testosterone on neuronal populations and their connections in a sensorimotor brain nucleus controlling song production in songbirds: a manganese enhanced-magnetic resonance imaging study. Neuroimage 21:914-923.
Voogd J (1998) Visual system. In: The Central Nervous System of Vertebrates (Nieuwenhuys R, Donkelaar HJ, Nicholson C, eds). New York: Springer.
Watanabe T, Michaelis T, Frahm J (2001) Mapping of retinal projections in the living rat using high-resolution 3D gradient-echo MRI with Mn^{2+}-induced contrast. Magn Reson Med 46:424-429.
Yamada M, Momoshima S, Masutani Y, Fujiyoshi K, Abe O, Nakamura M, Aoki S, Tamaoki N, Okano H (2008) Diffusion-tensor neuronal fiber tractography and manganese-enhanced MR imaging of primate visual pathway in the common marmoset: preliminary results. Radiology 249:855-864.
Zhang J, Hu YT, Sheng XL, Li Y, Ren J, Ma ZZ (2010a) Evaluation of toxicity of manganese ions to rabbit retina. Zhonghua Yan Ke Za Zhi 46:597-603.
Zhang P, Fa ZQ, Chang HG, Yang LJ, XU RX, Jiang XD (2010b) Dynamic manganese-enhanced functional magnetic resonance imaging on rat visual cortex. Zhonghua Shenjing Yixue Zazhi 9:128-132.

Copyedited by Slone-Murphy J, Hindle A, Yu J, Qiu Y, Li CH, Song LP, Zhao M